

Recent Developments and Validation of the Eulerian Lagrangian Fluid-Structure Code KOELSCH-2D

K. Gerling, L. Lange, I. Schlein

INTERATOM GmbH, Postfach, D-5060 Bergisch-Gladbach 1, Germany

Abstract

The concept and main features of the fluid-structure code system KOELSCH has been described previously [1] to be 1D-Eulerian-Lagrangian, 2D-Eulerian and 3D-Eulerian options for the treatment of hydrodynamics and essentially 2D-Lagrangian (cylindrical) coordinates processor of thin shell theory for structural dynamics. Important features were marker particle concept with continuous automatic rezoning, Eulerian substitute lines approximating Lagrangian lines (cutting Eulerian cells), assuring pure 2D-Eulerian hydrodynamics and quasi-1D-Eulerian-Lagrangian treatment for fluid between structures, lying close together.

Since the main goal of the code development is the advanced simulation of the mechanical loading and response of the primary containment of an LMFBR in case of an HCDA, emphasis was put on the application of the axi-symmetric KOELSCH-2D to reactor configurations. Recent developments and validation are presented here.

These are mainly concerned with fluid boundary movement near structures, e.g. the description of slug impact, the treatment of fluid sliding along structures.

As validation example the postcalculation of an explosion experiment in a 1/6-scaled reactor vessel model is presented comparing numerical and experimental results. For demonstration of the new code capabilities an HCDA in a large pool-type reactor vessel with a non-fixed plug is calculated; this could be interesting for risk oriented studies.

1. Introduction

The development of the code KOELSCH-2D was primarily directed to treat the mechanical consequences of a hypothetical core disruptive accident (HCDA) in a LMFBR [1]. In the future it may also serve as a basis for calculating the dynamic loading of steam generator components and internals in case of severe steam generator accidents producing pressure waves. KOELSCH-2D uses an Euler grid favourable for gross fluid transport phenomena without losing flexibility in searching for material and phase boundaries. This is performed by the concept of variable Eulerian substitute lines following marker particles in a definite Euler grid.

In fluid dynamics Euler and mass continuity equations are solved, using an explicit FD-integration scheme, modified by applying shape functions for density, pressure and velocity. In structure dynamics the shell theory is formulated with finite differences neglecting sublayers.

To get more flexibility in fluid boundary description various code expansions are implemented. Their application to representative test problems demonstrated their validity. In addition to problems in reactor technology (HCDA, steam or hydrogen explosion within pressure vessel) also similar tasks in other technical branches are solvable by KOELSCH-2D e.g. chemical explosions in containers filled with fluid, pressure wave propagation in solids and fluids.

2. Recent Developments

Euler-Lagrange Processor EULAMA

As described previously [1] EULAMA is used for the description of fluid dynamics between structures lying close together (Fig.1). In such cases a pure Euler description would require a mesh fine enough to guarantee a defined pressure in narrow fluid regions. To avoid such uneconomic Euler grids EULAMA performs the fluid dynamics locally by higher resolution in a flexible Euler-Lagrange representation. The theory presented earlier [1] is now expanded by a numerical diffusion term in the continuity equation

$$\dot{\xi} = \dot{\xi}_{\text{old}} - \lambda \nabla^2 \xi \quad (1)$$

to damp numerical oscillations.

The EULAMA subgrid must be coupled with the Euler grid. This is done by substituting the EULAMA cell queue by a polygonal line, which is treated in fluid dynamics like an ordinary shell.

Multiple Shell Connection Processor KNOTEN

To treat dynamics of multiple shell connections (MSC) the calculation scheme for simple shell elements must be modified. The impulse equation is written in integral form:

$$\int_V \rho \ddot{x} dV = \int_V \nabla \underline{\underline{\sigma}} dV \quad (3)$$

ρ = density of the MSC

\underline{x} = position vector in the MSC

V = volume of the MSC

$\underline{\underline{\sigma}}$ = stress tensor in the MSC

Using Gauss' principle the eq. (3) changes to

$$\int_V \rho \ddot{x} dV = \oint_A \underline{\underline{\sigma}} dA \quad (4)$$

The right hand side area integral will be performed over the surface of each shell connection branch (Fig.2 over shell No. 1 to 5).

This leads to a relationship for the center of mass of the MSC \underline{x}_0 :

$$\ddot{\underline{x}}_0 = \frac{1}{\rho} \sum_{k=1}^{N=\text{Numb. of branches}} \underline{\underline{F}}_k (\text{stress comp., } \Delta p) \quad (5)$$

This calculation procedure is independent of geometrical complexity of a structure connection, i.e. N may be any number greater than 1.

Code Expansions

Expansions made in existing code parts offer new capabilities especially in fluid structure coupling problems and fluid movement near structures.

Topology Matrix: During coupling structure and fluid motion information is required about the topological situation of structures and fluids relative to each other. To get this information the more complicated way of evaluating all coordinates is now substituted by using a topology matrix. Here, all topological relations are to be stored as input data. The matrix elements A_{jk} , $j, k=1 \dots$ number of shells, accept the values 2, 1, 0, -1, -2 meaning e.g. that line No. j is right from line No. k, or that the neighbourhood of lines j and k is not permitted at all. The introduction of the topology matrix reduces the calculation effort considerably and improves the logical code security.

Fluid Structure Touching: During slug impact of an HCDA in a LMFBR the coolant displaces the cover gas, approaches the roof, impacts and detaches from there. To describe this coolant movement marker particles are used driven by the Euler velocities of their nearest grid point.

Approach (Fig.3): If the distance is half a mesh size or less between marker and structure the driving fluid touches the structure in the Euler grid representation. Nevertheless the marker particle is driven as before and the locally displaced fluid influences this movement by its pressure.

Impact (Fig.4): The Euler cells under the structure now are filled with fluid producing the impact pressure until the fluid is stopped. During this phase marker particles reaching the structure are captured there. As long

as their driving Euler velocities are directed to the structure, only their tangential component is respected constraining the marker particle movement along the structure.

Detachment (Fig.5): As soon as the driving Euler velocity is redirected from structure to fluid, the captured marker particles come off the structure, while the cell pressure decreases, but not below the cover gas pressure. The displaced fluid reoccupies Euler cells with initial values for pressure and density taken from the next neighbour or in case of isolated reoccupation from its gasbag (Fig.6).

Gasbags (Fig.7): Volumes enclosed by marker particle lines and/or structure lines can be defined as gasbags i.e. homogeneous fluid filled volumes. Additional to analyzing capabilities, the time-dependent status of gasbags disposes initial values for pressure and density in case of the isolated reoccupation of displaced fluid regions e.g. cover gas reexpansion (Fig.6).

Fluid Sliding (Fig.8): The Euler grid in KOELSCH-2D has defined the velocities area-centered to the pressure points. So, the velocity can be calculated using a pressure gradient defined by the next four pressures. This concept must be modified for velocities an Eulerian substitute lines representing boundaries, because the associated pressures are separated by the boundary. Here, the velocity tangentially to the boundary is overtaken from the next neighbour for calculation of mass transport on both sides.

Code Modifications

During validation work some modifications were necessary concerning the calculation scheme in fluid dynamics, free motion of structures and code handling.

Upwind technique application: The transport term in the impulse equation for fluids is numerically formulated in full upwind expressions of first order. Especially impulse transport through perforated structures is influenced by this correction. Better agreement in validation problems could be achieved.

Non-fixed structures: Special situations require the calculation of non-fixed structures after failure of fixation. Here, the boundary conditions for free motion under gravitation and driving pressures are formulated.

Code handling: To guarantee easy code handling, a rigorous modular and optional code text structure is built up: Six modules and ca. 40 options offer adaption of the necessary program text to each problem situation.

3. Validation

Each code expansion and modification has been checked according to its logic and numerical effects on the results of validation examples.

Application of KOELSCH-2D on an explosion experiment in a reactor model

This experiment is described in previous publications, e.g. [2], so that we may limit explanations on KOELSCH-specific features, only.

In Fig.9 the experimental setup is compared to the KOELSCH-2D model. All important details are represented in the model except for the roof with hanging construction. Here, for simplification a rigid plate is postulated, which is also taken as the fixed reference in space.

The multiple structure connection processor KNOTEN enabled the calculation of complex structure points e.g. the connection grid plate/shield tank inlet plenum vessel. The Euler-Lagrange processor EULAMA permitted the treatment of enclosed water between spherical tank and inlet plenum vessel.

The description of the water hammer within the ring space and its following detachment was satisfied by the new fluid structure touching treatment. The definition of cover gas "air" as gasbag guaranteed its retarding influence just until all marker particles have reached the roof. Especially all upwind corrections played an important role. Without upwind formulation in the Euler equation, instabilities would stop the calculation near a great velocity divergence, e.g. in the shield tank upper region. Also the deflection of the shield tank in this region was described sufficiently only after introduction of the upwind formulation for the impulse transport through perforated structures.

The pressure and impulse histories on shield vessel and outer vessel calculated by KOELSCH-2D are compared to experimental results on Fig.10 and Fig.11. The agreement is pretty good. Fig.12 shows the experimental and numerical results for the circumferential strain profiles of the shield vessel and of the outer vessel. The agreement is also fairly good especially for the shield vessel. Concerning the discrepancies for the outer vessel it must be recalled that the vessel is assumed to be fixed in height of the cover plug. This prevents sliding of the vessel out of the cover plug region and reduces the maxima of the circumferential strain profile as well as shifts them to lower positions. In general, the comparison of the KOELSCH-2D calculation and the experiment demonstrates that the quality of the results is comparable to that obtained by other calculations also by Lagrangian codes [27].

Application of KOELSCH-2D to a large pool-type LMFBR

A modelization of a typical large LMFBR pool-type vessel with the most important internal structures is taken as a further application example. Background for this are HCDA risk investigations.

In Fig.13 the idealization of a large LMFBR pool-type reactor vessel is shown. Besides an outer and an inner tank, also the grid plate with support is represented. Within the roof the plug is assumed to be a plate without fixation anywhere allowing for the vertical motion after an explosive discharge within the core region.

The mostly applied code expansion is the fluid structure touching procedure. After slug impact the repeated touching and detaching of the flying and driving sodium is of special interest. Here, the reoccupation of cover gas cells under the plug as well as the compression of gas to very little

space under the fixed part of the roof has to be managed.

After reaching a definite height sodium can flow over the roof into the secondary containment. From this the radiological loading can be determined.

During the postulated high mechanical energy release the greatest energy part is consumed by plastification of steel (Fig.14, 15). The upper part of the outer vessel experiences the greatest deformation. The energy of motion of the flying plug is also considerable. The sodium discharge from the open system is limited by the bubble surface, which separates upper and lower sodium regions. These results depend on energy release assumptions rather critically.

4. Conclusions

After implementation of the new modules EULAMA and KNOTEN and after the realization of expansions and modifications concerning more complicated fluid structure ineractive motion the code KOELSCH-2D is applicable for suitable geometrical configurations within reactor accident analysis. But also similar tasks outside nuclear technology, e.g. explosions in a container filled with fluid, pressure wave propagation in solids and fluids can be calculated.

5. References

[1] Lange, L., Gerling, W., Schlein, I.
Paper B8/7 of 6th SMIRT-Conf., Paris 1981

[2] Bieselt, R., et al.
Paper E3/2 of 6th SMIRT-Conf., Paris 1981

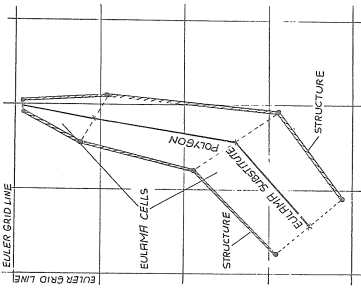


Fig. 1 EULAMA application

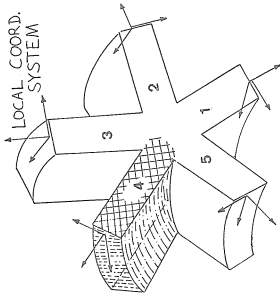


Fig. 2 KNOTEN element

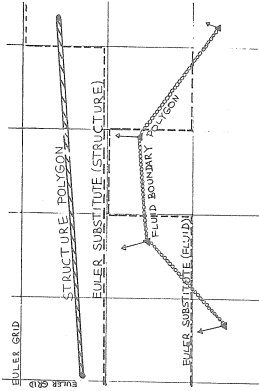


Fig. 3 Approach of fluid boundary to structure

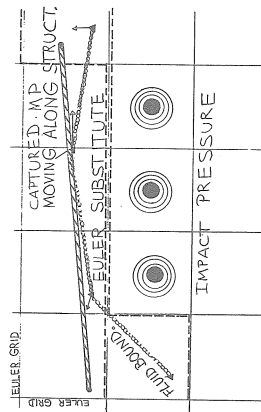


Fig. 4 Impact of fluid boundary to structure

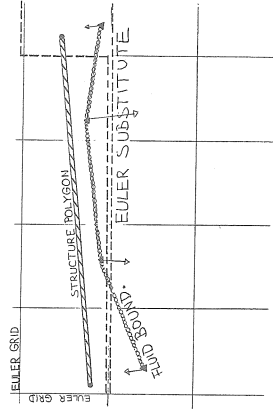


Fig. 5 Detachment of fluid boundary from structure

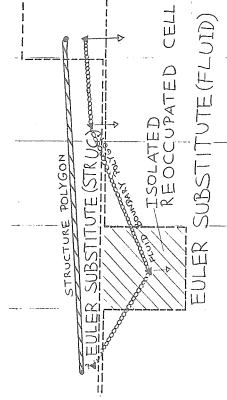


Fig. 6 Isolated reoccupation of an Euler cell

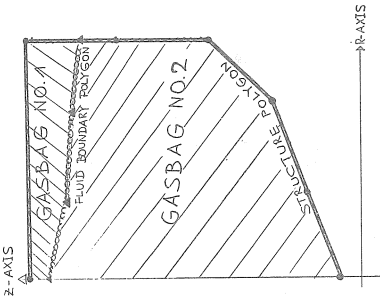


Fig. 7 Gasbags

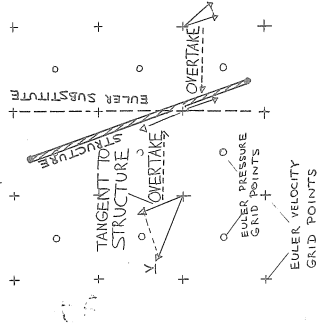


Fig. 8 Fluid sliding along structures.

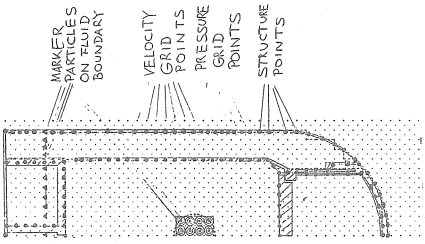


Fig. 9 Scaled reactor-vessel model.

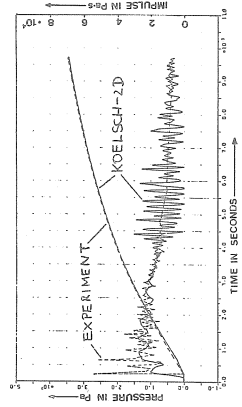


Fig. 10 Pressure and impulse on shield vessel at charge height

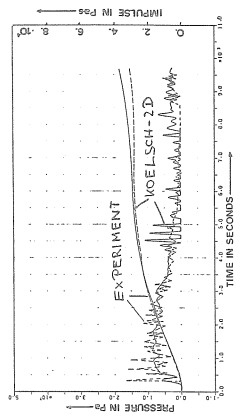


Fig. 11 Pressure and impulse on outer vessel at charge height

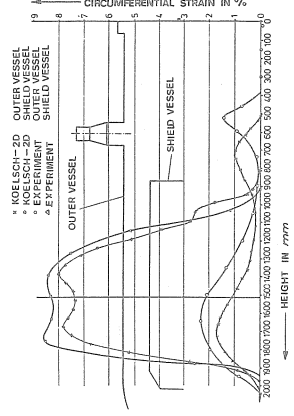


Fig. 12 Circumferential strain profiles

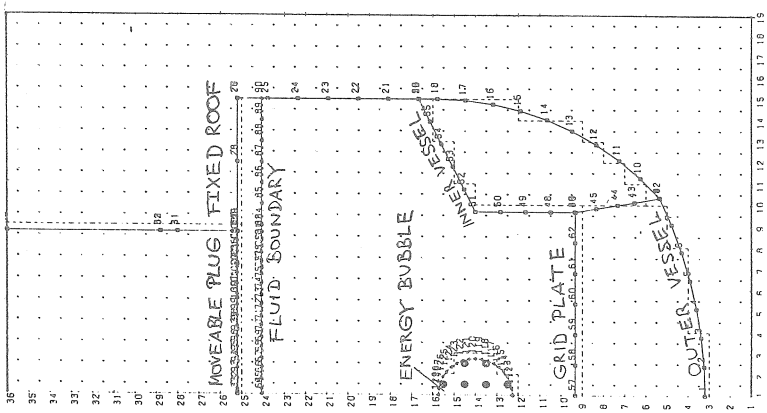


Fig. 13 Model of a LMFR pool-type reactor-vessel

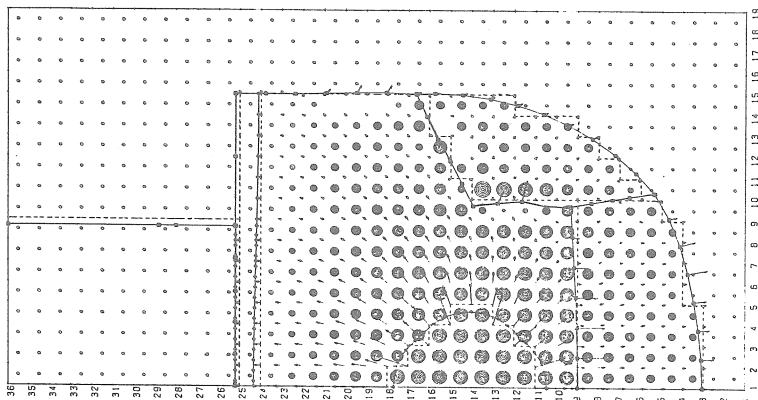


Fig. 14 KOELSCH-2D calculation after ca. 40 ms

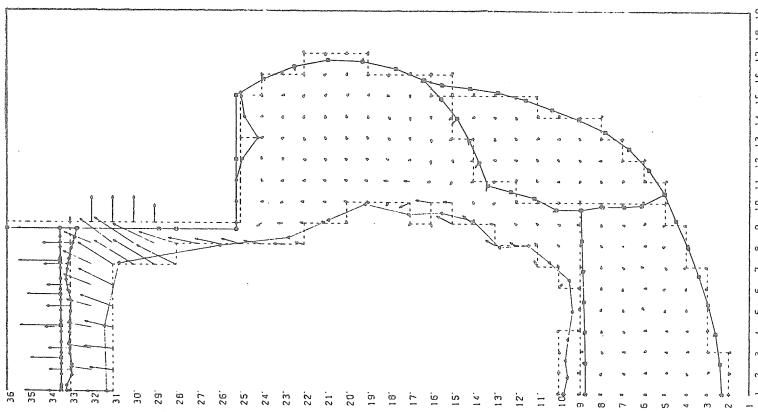


Fig. 15 KOELSCH-2D calculation after ca. 500 ms